Toward a Novel Metal-Based Chemotherapy against Tropical Diseases. 6. Synthesis and Characterization of New Copper(II) and Gold(I) Clotrimazole and Ketoconazole Complexes and Evaluation of Their Activity against *Trypanosoma cruzi*

Maribel Navarro,*,† Efren J. Cisneros-Fajardo,† Teresa Lehmann,† Roberto A. Sánchez-Delgado,*,† Reinaldo Atencio,† Pedro Silva,‡ Renee Lira,§ and Julio A. Urbina§

Chemistry, Physics, and Biophysics and Biochemistry Centers, Instituto Venezolano de Investigaciones Científicas (IVIC), Apartado 21827, Caracas 1020-A, Venezuela

Received March 21, 2001

The complexes $[Cu(CTZ)_4]Cl_2 \cdot 2H_2O$ (**1**), $[Cu(CTZ)Cl_2]_2$ (**2**), $[Cu(KTZ)_3Cl_2]$ (**3**), and $[Cu(KTZ)Cl_2]_2 \cdot 2H_2O$ (**4**) were prepared by reaction of $CuCl_2$ with CTZ and KTZ (where CTZ = 1-[[(2-chlorophenyl)diphenyl]methyl]-1*H*-imidazole and KTZ = *cis*-1-acetyl-4-[4-[[2-(2,4-dichlorophenyl)-2-(1*H*-imidazol-1-ylmethyl)-1,3-dioxolan-4-yl]methoxy]phenyl]piperazine), respectively, in acetonitrile at different ligand to metal molar ratios. Gold complexes $[Au(PPh_3)(CTZ)]PF_6$ (**5**) and $[Au(PPh_3)(KTZ)]PF_6 \cdot H_2O$ (**6**) were synthesized by reaction of $AuClPPh_3$, with KPF_6 and CTZ or KTZ in acetonitrile. All the new compounds were characterized by NMR spectroscopy and microanalytical methods, and for the paramagnetic species EPR spectroscopy and DC magnetic susceptibility measurements were also employed. The solid-state structure of **1** has been determined by X-ray crystallography. **1** crystallizes in the triclinic space group $P\bar{1}$, with $a = 12.773(2)$ Å, $b = 15.326(4)$ Å, $c = 11.641(2)$ Å, $V = 1957.4(7)$ Å^3, $Z = 1$, and $D_{calcd} = 1.284$ g/cm^3. The structure refinement converged at R1 = 0.0731 and wR2 = 0.1962. Complex **1** displayed a square-planar structure typical for tetrakis(imidazole)copper(II) complexes. The new compounds were tested for in vitro activity against cultures of epimastigotes of *Trypanosoma cruzi*, the causative agent of Chagas disease. At concentrations equivalent to 10^{-6} M of total CTZ or KTZ (in DMSO) all the complexes exhibited significantly higher growth inhibitory activity than their respective parental compounds.

Introduction

Trypanosoma cruzi is the causative agent of Chagas disease, an illness which currently afflicts over 17 million people in Latin America and ranks as the third largest parasitic disease worldwide after malaria and schistosomiasis.[1] Despite recent achievements in the understanding of the biochemistry of *T. cruzi*,[2] specific chemotherapy of Chagas disease is still very unsatisfactory as currently available drugs have very limited activity in the prevalent chronic phase of the disease and have common toxic side effects, which can lead to discontinuation of treatment.[1,2]

In our search for new drugs that combine a high activity with a low toxicity, we have been using a novel strategy based on the fact that coordination of organic compounds such as CTZ and KTZ, with known anti *T. cruzi* activity, to transition metals, such as Ru, Rh, Cu, Au, and Pt, may result in a remarkable enhancement of the biological activity.[3]

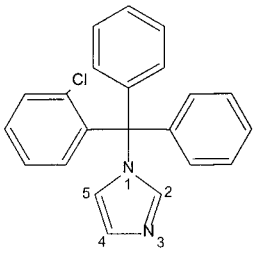

CTZ

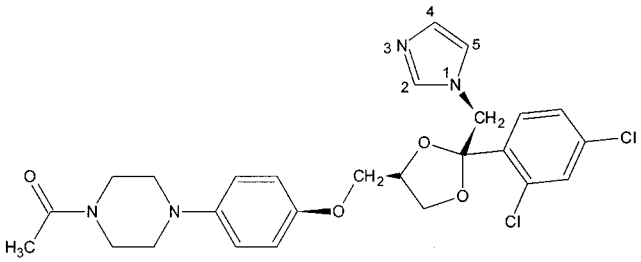

KTZ

In this paper, we report a new series of copper and gold complexes of these two ligands. Various copper complexes have

* Corresponding authors. Phone: (58-212) 5041642. Fax: (58-212) 5041350. E-mail address: mnavarro@ivic.ve.
† Chemistry Center.
‡ Physics Center.
§ Biophysics and Biochemistry Center.

(1) *World Bank, World Development Report 1993*: *Investing in Health*; Oxford University Press: Oxford, U.K., 1993.
(2) (a) Urbina, J. A.; Payares, G.; Molina, J.; Sanoja, C.; Liendo, A.; Lazardi, K.; Piras, M. M.; Piras, R.; Pérez, N.; Wincker, P.; Ryley J. F.; *Science* **1996**, *273*, 969. (b) Urbina, J. A.; Lazardi, K.; Aguirre, T.; Piras, M. M.; Piras, R. *Antimicrob. Agents Chemother*. **1998**, *32*, 1237. (c) Lazardi, K.; Urbina, J. A.; De Souza, W. *Antimicrob. Agents Chemother*. **1990**, *34*, 2097. (d) Urbina, J. A.; Lazardi, K.; Aguirre, M.; Piras, M. M.; Piras, R. *Antimicrob. Agents Chemother*. **1991**, *35*, 730. (e) Urbina, J. A.; Lazardi, K.; Marchan, E.; Visbal, G.; Aguirre, M.; Piras, M. M.; Piras, R.; Maldonado, R. A.; Payares, G.; De Souza, W. *Antimicrob. Agents Chemother*. **1993**, *7*, 580. (f) Maldonado, R. A.; Molina, J.; Payares, G.; Urbina, J. A. *Antimicrob. Agents Chemother*. **1993**, *37*, 1353. (g) Urbina, J. A.; Vivas, J.; Visbal, G.; Contreras, L. M.; *Mol. Biochem. Parasitol.* **1995**, *73*, 199. (h) Urbina, J. A.; Vivas, J.; Lazardi, K.; Molina, J.; Payares, G.; Piras, M. M.; Piras, R. *Chemotherapy* **1996**, *42*, 1294.

10.1021/ic0103087 CCC: $20.00
Published on Web 12/06/2001

been reported to inhibit bacterial, fungal, yeast, algal, mycoplasma, and viral growth.[4] Copper derivatives have also been employed in the treatment of inflamation.[5] Gold complexes in turn have long been used in the treatment of various other diseases such as rheumatoid arthritis (aurothiomalate and aurothioglucose complexes) and tuberculosis (cyanide and thiosulfate derivatives).[6] The complex auranofin [(*s*)-2,3,4,5-tetraacetyl-1-*β*-*O*-thioglucose(trietilphosphine)gold(I)] has also proved to be active against P388 lukemia.[7] In contrast, the potential of copper and gold derivatives as antiparasitic agents has so far been little explored.[6f,9]

In our laboratory we have found that copper−chloroquine[8] and gold−chloroquine[9] complexes are active against malaria parasites. Continuing our efforts to develop new anti *T. cruzi* agents, we now report the coordination of CTZ and KTZ to copper and gold ions to yield new Cu(II)−CTZ and Cu(II)−KTZ as well as Au(I)−CTZ and Au(I)−KTZ complexes. The characterization of these complexes was achieved through NMR, EPR, χ_{dc}, IR, UV−vis, elemental analysis, and, in the case of **1,** also an X-ray diffraction study. The biological activities of these complexes against the epimastigote form of *T. cruzi* were also evaluated indicating that all of them inhibit the proliferation of the parasite. The results are compared with other previously reported metal−CTZ, and −KTZ complexes.[3]

Experimental Section

General Procedure. Solvents of analytical grade were distilled from appropriate drying agents prior to use. CTZ, KTZ, $AuClPPh_3$, and $CuCl_2$ were used as obtained without purification. Elemental analyses were performed at the Chemistry Center (IVIC) on a Fisons analyzer EA 1108. IR spectra were recorded on a Nicolet 5DCX FT spectrometer, while UV−vis spectra were recorded on a HP 8453 diode array instrument using chloroform solutions (10^{-3} M) of the complexes.

$[Cu(CTZ)_4]Cl_2 \cdot 0.66CH_2Cl_2$ (1). $CuCl_2$ (332 mg; 2.47 mmol) was dissolved in acetonitrile (35 mL), and CTZ (1.629 mg; 4.97 mmol) was added to the solution which was stirred under reflux in a nitrogen atmosphere for 1 h. The volume of the solvent was reduced until precipitation began, and the mixture was allowed to stand overnight at −10 °C, after which the blue solid obtained was filtered off, washed with diethyl ether, and dried under vacuum (yield, 1550 mg, 41% with respect to Cu). Anal. Calcd for $C_{88.66}H_{69.32}Cl_{7.32}N_8Cu$: C, 67.82; H, 4.42; N, 7.14. Found: C, 67.76; H, 5.08; N, 6.69. IR (cm^{-1}): ν(C═C) 1492, ν(C═N) 1443. λ_{max} ($CHCl_3$, 10^{-3} M) = 290 nm, 741 nm.

$[Cu(CTZ)Cl_2]_2$ (2). $CuCl_2$ (52 mg; 0.387 mmol) was dissolved in acetonitrile (15 mL), CTZ (131 mg; 0.380 mmol) was added to the solution which was stirred at room temperature for 1 h. The volume of the solvent was reduced until precipitation began, and the mixture was allowed to stand overnight at −10 °C, after which the green solid was obtained was filtered off, washed with diethyl ether, and dried under vacuum (yield, 123 mg, 66%). Anal. Calcd for $C_{44}H_{34}Cl_6N_4Cu_2$: C, 55.06; H, 3.55; N, 5.84. Found: C, 55.29; H, 3.72; N, 5.65. IR (cm^{-1}): ν(C═C) 1491, ν(C═N) 1448. λ_{max} ($CHCl_3$, 10^{-3} M) = 241 nm, 293 nm. ^{1}H NMR ($CDCl_3$; δ, ppm): 46.5 (s, 1H); 40.1 (s, 1H); 38.0 (s, 1H).

$[Cu(KTZ)_3Cl_2]$ (3). $CuCl_2$ (50 mg; 0.370 mmol) was dissolved in acetonitrile (15 mL). KTZ (810 mg; 1.53 mmol) was added to the solution which was stirred at room temperature under a nitrogen atmosphere for 1 h. The volume of the solution was reduced by 70%. Ethanol was added, and the mixture was allowed to stand overnight at −10 °C. The blue solid obtained was filtered off, washed with diethyl ether, and dried under vacuum (yield, 414 mg, 65%). Anal. Calcd for $C_{78}H_{84}Cl_4N_{12}O_{12}Cu$: C, 53.50; H, 5.14; N, 9.60. Found: C, 53.65; H, 4.97; N, 9.49. IR (cm^{-1}): ν(C═C) 1510, ν(C═N) 1439. λ_{max} ($CHCl_3$, 10^{-3} M) = 299, 656, 796 nm.

$[Cu(KTZ)Cl_2]_2 \cdot 2H_2O$ (4). $CuCl_2$ (22 mg; 0.15 mmol) was dissolved in freshly distilled acetonitrile (10 mL). KTZ (80 mg; 0.15 mmol) was added to the solution, which was stirred and kept under reflux in a nitrogen atmosphere for 1 h. The solvent was removed under vacuum, and the red solid obtained was redissolved in acetone (3 mL). The solution was filtered and precipitated with diethyl ether, and the mixture was allowed to stand overnight at −10 °C. The red solid obtained was filtered off, washed with ether diethyl, and dried under vacuum (yield, 63 mg, 61%). Anal. Calcd for $C_{52}H_{56}Cl_4N_8O_8Cu_2 \cdot 2H_2O$: C, 45.64; H, 4.39; N, 8.19. Found: C, 45.44; H, 4.05; N, 7.87. IR (cm^{-1}): ν(C═C) 1510, ν(C═N) 1435. λ_{max} ($CHCl_3$, 10^{-3} M) = 262 nm, 485 nm. ^{1}H NMR ($CDCl_3$; δ, ppm): 46.5 (s, 1H); 39.8 (s, 1H); 37.0 (s, 1H).

$[Au(CTZ)(PPh_3)]PF_6$ (5). A suspension of $AuClPPh_3$ (100 mg; 0.20 mmol) in acetonitrile (25 mL) was refluxed under nitrogen until complete dissolution. KPF_6 (273 mg; 1.48 mmol) was added, and refluxing was continued for 2 h. CTZ (108 mg; 0.31 mmol) was added. The mixture was stirred and refluxed for 24 h and then cooled to room temperature and filtered through Celite. The volume of the solvent was reduced under a nitrogen stream, and diethyl ether was added until the solution became turbid. On cooling of the sample to −10 °C overnight, a white product precipitated. It was filtered off, washed with water and diethyl ether, and dried under vacuum (yield, 46 mg, 24%). Anal. Calcd for $C_{40}H_{32}ClF_6N_2P_2Au$: C, 47.0; H, 3.92; N, 2.74. Found: C, 46.9; H, 3.34; N, 2.73. IR (cm^{-1}): ν(C═C)1500, ν(C═N) 1435, ν(P−F) 843. λ_{max} ($CHCl_3$, 10^{-4} M) = 248 nm. ^{1}H NMR ($CDCl_3$; δ, ppm): 7.91 (s, 1H); 7.54 (m, 15H, PPh_3); 7.36 (m, 9H); 7.13 (m, 4H); 7.01 (m, 2H). ^{31}P {^{1}H}NMR ($CDCl_3$; δ, ppm): 27.9 (s, PPh_3); 146 (hep, PF_6).

$[Au(KTZ)(PPh_3)]PF_6 \cdot 2H_2O$ (6). A suspension of $AuClPPh_3$ (155 mg; 0.31 mmol) in acetonitrile (25 mL) was refluxed under nitrogen until complete dissolution. KPF_6 (230 mg; 1.25 mmol) was added, and refluxing was continued for 2 h. KTZ (166 mg; 0.31 mmol) was added, and the mixture was stirred and refluxed for 24 h, cooled to room temperature, and then filtered through Celite. The solution was dried, and the solid was dissolved in acetone (3 mL). The solution was filtered, and a white solid was made to precipitate by the addition of diethyl ether; then it was filtered off, washed with water and diethyl ether, and dried under vacuum (yield, 221 mg, 59%). Anal. Calcd for $C_{44}H_{43}Cl_2F_6N_4P_2Au \cdot 2H_2O$: C, 45.1; H, 3.67; N, 4.78. Found: C, 45.0; H, 3.87; N, 4.37. IR (cm^{-1}): ν(C═C) 1517, ν(C═N) 1445. λ_{max} ($CHCl_3$, 10^{-4} M) = 250, 298 nm. ^{1}H NMR ($CDCl_3$; δ, ppm): 8.24 (s, 1H); 7.62 (d, J = 9.0 Hz, 1H); 7.54 (m, 15H, PPh_3); 7.43 (d, J = 2.1 Hz, 1H); 7.28 (m, 1H); 7.20 (s, 1H); 7.06 (s, 1H); 6.77 (AA′XX′, 4H); 4.59 (AB, 2H); 4.33 (m, 1H); 3.75 (m, 6H); 3.52 (m, 2H); 2.85 (m, 4H); 2.10 (s, 3H); 1.67 (s, H_2O). ^{31}P {^{1}H}NMR ($CDCl_3$; δ, ppm): 28.2 (s, PPh_3); 146 (hep, PF_6).

(3) (a) Sánchez-Delgado, R. A.; Lazardi, K.; Rincón, L.; Urbina, J. A.; Hubert, A. J.; Noels, A. F. *J. Med. Chem.* **1993**, *36*, 2041. (b) Sánchez-Delgado, R. A.; Navarro, M.; Lazardi, K.; Atencio, R.; Capparelli, M.; Vargas, F.; Urbina, J. A.; Bouillez, A.; Hubert, A. J.; Noels, A. F. *Inorg. Chim. Acta* **1998**, *275*−*276*, 528−540. (c) Navarro, M.; Lehmann, T.; Cisneros-Fajardo, E. J.; Fuentes, A.; Sanchez-Delgado, R. A.; Silva, P.; Urbina, J. A. *Polyhedron* **2000**, *19*, 2319−2325.

(4) Carcelli, M.; Mazza, P.; Pelizzi, C.; Zani, F. *J. Inorg. Biochem.* **1995**, *15*, 188−222.

(5) (a) Adams, S.; Cobb, R. *Prog. Med. Chem.* **1976**, *5*, 59−138. (b) Sorenson, J. R. *Inflamatory Diseases and Cooper*, 1st ed.; Humana Press: Clifton, NJ, 1982. (c) Sorenson, J. R. J. *Prog. Med. Chem.* **1989**, *26*, 437. (d) Sorenson, J. R. J. A *Physiological Basis for Pharmacological Activities of cooper complexes: An hypothesis*; Humana Press: Clifton, NJ, 1987; pp 3−16, 43, 57. (g) West, D. X.; Thientanavanich, I.; Liberta, A. E. *Trans. Met. Chem.* **1995**, *20*, 303. (h) Liberta, A. E.; West, D. X. *BioMetals* **1992**, *5*, 121.

(6) (a) Farrell, N. Transition Metal Complexes as Drugs and Chemotherapeutic Agents. In *Catalysis by Metal Complexes*; James, B. R.R, Ugo, R., Eds.; Kluwer: Dordrecht, The Netherlands, 1989; Chapter 11 and references therein. (b) Rhodes, M. D.; Sadler, P. J.; Scawen, M. D.; Silver, S. *J. Inorg. Biochem.* **1992**, *46*, 129. (c) Brown, D. H.; Smith, W. E. *Chem. Soc. Rev.* **1980**, *9*, 217. (d) Cofer, M. T., Shaw, C. F., III. *Inorg. Chem.* **1986**, *25*, 333. (e) Aaseth, J.; Haugen, M.; Forre, O. *Analyst* **1998**, *123*, 3−6. (f) Shaw, C. F., III. *Chem. Rev.* **1999**, *99*, 2589.

(7) Mirabelli, C. K.; Johnson, R. K.; Song, C. M.; Fancette L.; Muirhead, K.; Crooke, S. T. *Cancer Res.* **1985**, *45*, 32.

(8) Navarro, M.; Sánchez-Delgado, R. A.; Pérez H. Unpublished results.

(9) Navarro, M.; Pérez, H.; Sánchez-Delgado, R. A. *J. Med. Chem.* **1997**, *40*, 1937.

Magnetic Measurements. EPR spectra were measured at room temperature in a Varian E-line spectrometer working in the X-band (ν = 9.3 GHz) with a homemade cylindrical cavity and a coaxial microwave coupler for the X-band. Experimental conditions (microwave power and modulation field) were adjusted to avoid saturation of signal intensity. DC magnetic susceptibility measurements were carried out in a computerized Faraday balance in the temperature range $76 \le T \le 250$ K; diamagnetic corrections of constituent atoms and temperature-independent paramagnetism were taken into account in our results. The χ_m^{-1} vs T curve is obtained from the experiment, and the μ_{eff} is calculated from the Curie constant C of the Cure−Weiss law[10]

$$\chi = \frac{C}{T - \Theta}$$

where

$$C = \frac{Ng^2\mu_B{}^2S(S+1)}{3K_B} \quad \mu_{eff}{}^2 \equiv g^2\mu_B{}^2S(S+1)$$

From this

$$\mu_{eff} = 2.827\sqrt{C_M}$$

N is the number of paramagnetic species per gram of sample, K_B is the Boltzman constant, C_M is the molar Curie constant, and Θ is the Curie temperature.

NMR Spectroscopy. NMR spectra were obtained in DMSO-d_6 solutions in a Bruker AVANCE500 spectrometer, ^{1}H NMR shifts being recorded relative to residual resonance in the deuterated solvent. For the paramagnetic complexes the NMR spectra were obtained using a 90^o pulse of 10 μs. An inversion−recovery pulse sequence (180^o −τ−90^o−Aq) was used to obtain nonselective proton longitudinal relaxation times (T_1) with the carrier frequency set at different positions to ensure the validity of the measurements. Signal: noise ratios were improved by applying a line-broadening factor of 30 Hz to the FID prior to Fourier transformation.

X-ray Crystallography. A blue-purple irregular crystal of dimensions 0.43 × 0.30 × 0.16 mm of **1** was mounted on a Rigaku AFC7S diffractometer with graphite-monochromated Mo Kα radiation. Cell constants and an orientation matrix for data collection were obtained from 25 centered reflections (range: 20° < 2θ < 31°). Data were collected at rt (room temperature) using the ω−2θ scan technique to a maximum 2θ value of 50°. A total of 3 standard reflections were measured for orientation and intensity control. No decay was noticed. Intensity data were corrected for Lorentz−polarization effects, and a semiempirical absorption correction was carried out on Ψ-scan measurements.[11] Of the 7236 reflections that were collected, 6896 were unique. The structure was solved by direct methods[12] and expanded using Fourier techniques. The full-matrix least-squares refinement[13] was based on F^2. All non-hydrogen atoms were refined anisotropically, except for those of the disordered dichloromethane solvent molecule, which was refined constraining the isotropic displacement parameters to be the same (0.12 Å^2) for the three non-hydrogen atoms. Preliminary refinement of the occupancy of this molecule converged to approximately 33%, so it was fixed to this value for subsequent refinements. Hydrogen atoms for this molecule were not included. Atomic scattering factors were those reported by Cromer and Waber[14] with anomalous dispersion correction.[15] Crystallographic details are collected in Table 1. Final atomic coordinates with equivalent isotropic displacement parameters and listings of atomic coordinates of the hydrogen atoms, anisotropic displacement parameters, and structure factors are available as Supporting Information.

Table 1. Crystallographic Data for **1**

empirical formula	$C_{88.66}H_{69.32}C_{17.32}CuN_8$
fw	1585.8
cryst color, habit	blue-purple, irregular
cryst dimens (mm)	0.43 × 0.30 × 0.16
cryst syst	triclinic
no. of reflcns used for unit cell determn (2θ range)	25 (20−31°)
space group	$P\bar{1}$
formula units/unit cell	1
a (Å)	12.773(2)
b (Å)	15.326(4)
c (Å)	11.641(2)
α (deg)	110.43(2)
β (deg)	100.67(2)
γ (deg)	66.62(2)
V (Å^3)	1957.4(7)
D_{calcd} (g/cm^3)	1.345
F_{000}	819
μ(Mo Kα) (cm^{-1})	5.34
difractometer	Rigaku AFC7S
radiation (λ, Å)	Mo Kα (0.710 69)
T (K)	293 (2)
2θ range (deg)	$1.5 \le 2\theta \le 25$
range of h, k, l	0 → 15, 16 → 18, 13 → 13
no. of reflcns measd	7236
no. of unique reflcns	6896
no. of obsd reflcns	3967
no. of params varied	476
weighting scheme	$[(\sigma F_0)^2 + (0.1088P)^2 + 0.5276P]^{-1}$, where $P = (F_0^2 + 2F_c^2)/3$
S(GOF)	1.173
R1[a] [$I > 2\sigma(I)$]	0.0706
wR2[b] [$I > 2\sigma(I)$]	0.1783
largest feature final diff map (e Å^{-3})	0.002

[a] $R1 = \sum||F_o| - |F_c||/\sum|F_o|$. [b] $wR2 = \{\sum[w(F_o^2 - F_c^2)^2]/\sum[w(F_o^2)^2]\}^{1/2}$.

Biological Tests against Epimastigotes of *T. cruzi*. Tests were conducted by following a previously reported method.[16] The EP stock of the epimastigote[17] form of *T. cruzi* was used throughout this study. The epimastigotes were cultured in liver infusion−tryptose medium supplemented with 10% calf serum at 28 °C with strong stirring (120 rpm) as previously described. The cultures were initiated with a cell density of 2 × 10^6 epimastigotes/mL. CTZ, KTZ, and compounds **1**−**6** were added as DMSO solutions (all concentrations corresponding to 10^{-6} M of the free CTZ or KTZ ligand) when the culture reached a cellular density of 10^7 epimastigotes/mL. Parasite proliferation was followed daily by the use of an electronic particle counter (model ZBI; counter Electronics, Inc, Hialeah, FL) and by direct counting with an hemacytometer. Controls (nontreated) cultures contained an equivalent amount of the solvent used to deliver the experimental compounds to the growth medium (1% v/v of dimethyl sulfoxide); at this concentration the solvent had no effects on cell viability or proliferation.

Safety Note. Handling of live *T. cruzi* was done according to established guidelines[18]

Results and Discussion

Synthesis and Characterization of Copper Complexes. The copper complexes were synthesized from $CuCl_2$ by reaction with

(10) McMillan, J. A. *Electron Paramagnetism Chemical Series*; Organization of American States (OAS): Washington, DC, 1975; No. 14.
(11) North, A. T. C.; Phillips, D. C.; Mathews, F. S. *Acta Crystallogr., Sect. A* **1968**, *24*, 351.
(12) *TEXSAN: Single-Crystal Structure Analysis Software*, version 1.6; Molecular Structure: The Woodlands, TX, **1993**.
(13) Sheldrick, G. M. *SHELXTL*, release 5.03; Siemens Analytical X-ray Instruments Inc.: Madison, WI, 1994.
(14) Cromer, D. T.; Waber, J. T. *Acta Crystallogr.* **1965**, *18*, 104.
(15) *International Tables of Crystallography*; Kynoch: Birmingham, England, 1974; Vol. 4.
(16) Lazardi, K.; Urbina, J. A.; De Sousa, W. *Antimicrob. Agents Chemother.* **1990**, *34*, 2097.
(17) Epimastigote: one of the proliferative stages of the parasite, equivalent to that present in its insect vector. Although this form is noninfective for vertebrates, it has many biochemical similarities with the infective (intracellular amastigote) form present in vertebrates and is commonly used in preliminary drug testing against this organism.
(18) Hudson, L.; F. Grover, W. E.; Gutteridge, R. A.; Klein, W.; Peters, R. A.; Neal, M. A.; Miles M. T.; Scott, R.; Nourish and B. P. Ager. *Trans. R. Soc. Trop. Med. Hyg.* **1983**, *77*, 416−419.

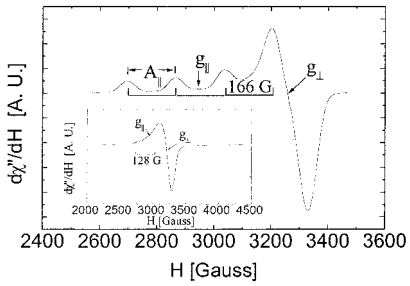

Figure 1. EPR spectrum for $[Cu(KTZ)_3Cl_2]$ showing the spectral parameters. The inset shows the broadened EPR spectrum for $[Cu(KTZ)Cl_2]_2$.

Table 2. EPR Spectroscopic Data for the Cu(II) Complexes

complex	$g_{\|\|}$	$g_\perp$	A (G)	μ_{eff} (μ_B)
$[Cu(CTZ)_4]Cl_2$ (**1**)	2.25	2.05	85	2.10
$[Cu(CTZ)Cl_2]_2$ (**2**)	2.25	2.06	141	2.12
$[Cu(KTZ)_3Cl_2]$ (**3**)	2.26	2.05	166	0.64
$[Cu(KTZ)Cl_2]_2$ (**4**)	2.27	2.08	128	1.92

CTZ or KTZ at different molar ratios. Compounds **1** and **3** were obtained by using an excess of the ligand, while **2** and **4** were obtained with a 1:1 copper to ligand molar ratio.

EPR Spectra and Magnetic Moment Data. The EPR spectra of powdered complexes **1**−**4** exhibit resolved features with $g_{||} > g_\perp$, consistent with a tetragonally elongated structure; a representative set of spectra, corresponding to **3** and **4**, is shown in Figure 1, and the EPR parameters for all compounds are shown in Table 2. All g values and spectra are characteristic of Cu(II) with axial symmetry.[19]

Complexes **1** and **3** show well-resolved signals due to the hyperfine splitting. For complex **1**, the low value of the hyperfine-coupling constant is indicative of the low electron density at the copper site and the freedom of movement in the copper plane. Additionally, the low intensity of the hyperfine signals can be taken as evidence of the unpaired electron spending a long time in the copper plane. The EPR spectrum of **3**, in turn, shows several well-defined narrow signals due to hyperfine splitting, which, in addition to the values obtained for the parameters of the spectrum, leads us to propose a monomeric structure for both of these compounds, as was confirmed by X-ray diffraction for **1** (vide infra). The EPR spectra for **2** and **4** showed a set of broadened hyperfine signals and an increment of the g values; this is an evidence of an increase dipolar interaction between paramagnetic ions and suggests the presence of more than 1 copper atom/molecule in these compounds.[20]

All the complexes obey the Curie−Weiss law in the temperature range $76 < T < 250$ K, and the values for μ_{eff} are shown in Table 2. The μ_{eff} values obtained for **1** and **3** are 2.10 and 0.64, respectively. Complex **1** shows a normal value of μ_{eff} for Cu(II); however, the μ_{eff} value for **3** is very low, which can be taken as indicative of a strong diamagnetic shielding from the environment (KTZ) around the metal ion. The μ_{eff} values obtained for **2** and **4** are 2.12 and 1.92, also normal for Cu(II) complexes. These results are in good agreement with those obtained from NMR experiments.

NMR Spectra. The NMR spectra of complexes **1**−**4** are shown in Figure 2. Complexes **1** and **3** do not show sharp isotropically shifted signals; this is in agreement with mononuclear Cu(II) structures and coherent with the magnetic and EPR data. The extremely large line widths of the NMR signals derived from the paramagnetic protons in these complexes make their detection impossible.[21,22] On the other hand, the spectra of complexes **2** and **4** exhibit reasonably sharp, isotropically shifted signals. The most likely reason for that is the presence in these complexes of two paramagnetic Cu(II) centers in each complex, which is known to produce effective relaxation mechanisms.[23−25] The NMR spectrum of **2** displays isotropically shifted signals at 46.5 ppm (T_1 = 3.97 ms), 40.2 ppm (T_1 = 5.77 ms), and 38.0 ppm (T_1 = 32.5 ms). Similarly, the isotropically shifted signals from the protons in **4** are located at 46.5, 39.8, and 37.1 ppm with relaxation times of 4.0, 5.8, and 18.0 ms, respectively. Since most probably in these complexes the KTZ and CTZ ligands bind to the Cu(II) ions through N3, the signals located at 46.5 and 40.2 ppm for **2** and 46.5 and 39.8 ppm for **4** can be tentatively assigned to the H2 and/or H4 protons, on the basis of NMR spectra of other dicopper(II) complexes containing imidazole ligands reported previously.[21] Unfortunately, due to the similar location of these protons with respect to the metal centers in **2** and **4** definitive assignments of these signals to specific protons cannot be performed without deuteration of the CTZ and KTZ ligands in the H2 and H4 positions. On the other hand, the signals at 38.0 ppm (**2**) and 37.0 ppm (**4**) can be confidently assigned to the H5 protons in CTZ and KTZ, respectively. This imidazole proton is the one located furthest away from the Cu(II) centers, and therefore, it is the least affected by the paramagnetic influence of the metal center; as a result, the H5 proton resonances are the least broadened which is reflected in their relatively long relaxation times (32.5 ms in **2** and 18.0 ms in **4**).

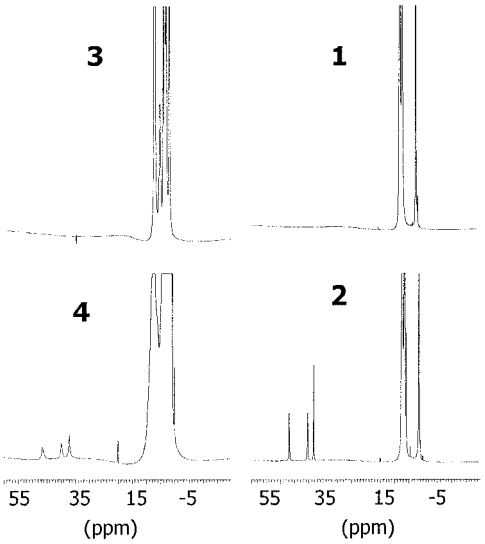

Figure 2. ^{1}H NMR spectra of the copper complexes **1**−**4**. In these spectra it is noteworthy the presence of signals at very low field for **2** and **4** (dimeric complexes), while **1** and **3** (monomeric complexes) do not show sharp isotropically shifted signals.

(19) (a) Sushil, K.; Misra; Chunzheng, W. *Magn. Reson. Rev.* **1990**, *14*, 157. (b) Newton, L. D. F.; Yoshitaka, G. *J. Mol. Struct. (THEOCHEM).* **1995**, 335, 175.
(20) (a) Boas, J. F.; Pilbrow, J. R. *J. Chem. Soc. A* **1969**, 721. (b) Bellitto, C.; Bigoli, F.; Deplano, P.; Mercuri M. L.; Pellinghelli, M. A.; Staulo, G.; Trogo, E. F. *Inorg. Chem.* **1994**, *33*, 3005.
(21) Maekawa, M.; Kitagawa, S.; Munakata, M.; Masuda, H. *Inorg. Chem.* **1989**, *28*, 1904.
(22) Bertini, I.; Turano, P.; Vila, A. J. *J. Chem. Rev.* **1993**, *98*, 2833.
(23) Satcher, J. H.; Balch, A. L. *Inorg. Chem.* **1995**, *34*, 3371.
(24) Holz, R. C.; Brink, J. M.; Gobena, F. T.; O'Connor, C. J. *Inorg. Chem.* **1994**, *33*, 6086.
(25) Kitajima, N.; Fijusawa, K.; Fujimoto, C.; Moro-oko, Y.; Hashimoto, S.; Kitagawa, T.; Toriumi, K.; Tatsumi, K.; Nakamura, A. *J. Am. Chem. Soc.* **1992**, *114*, 1277.

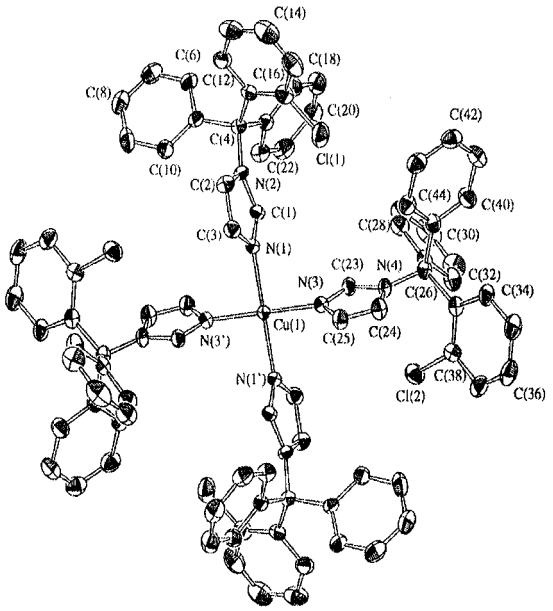

Figure 3. Molecular diagram (35% displacement ellipsoids) of the cation of **1** showing the atom-numbering scheme. Prime atom labels are generated by a center of symmetry.

Table 3. Selected Bond Distances (Å) and Angles (deg) for **1**

Cu−N(1)	2.013(4)	N(3)−C(23)	1.316(7)
Cu−N(3)	1.996(4)	N(3)−C(25)	1.382(7)
Cu−Cl	2.998	N(4)−C(24)	1.377(7)
N(1)−C(1)	1.297(7)	N(4)−C(26)	1.486(7)
N(1)−C(3)	1.373(7)	N(4)−C(23)	1.344(7)
N(2)−C(2)	1.381(7)	C(2)−C(3)	1.344(7)
N(2)−C(4)	1.491(6)	C(24)−C(25)	1.335(8)
N(2)−C(1)	1.357(6)		
N(1)−Cu−N(3′)	88.0(2)	C(1)−N(1)−C(3)	106.8(4)
N(1)−Cu−N(3)	92.0(2)	C(1)−N(2)−C(2)	105.3(4)
N(1)−C(1)−N(3)	111.8(5)	C(1)−N(2)−C(4)	130.0(4)
N(2)−C(2)−C(3)	107.6(5)	C(2)−C(3)−N(1)	108.5(5)
N(3)−C(23)−N(4)	111.6(5)	C(2)−N(2)−C(4)	124.7(5)
N(4)−C(24)−C(25)	107.2(5)	C(23)−N(4)−C(24)	106.3(5)
Cu−N(1)−C(1)	124.7(4)	C(23)−N(4)−C(26)	130.0(5)
Cu−N(1)−C(3)	127.25(4)	C(24)−C(25)−N(3)	109.4(5)
Cu−N(3)−C(23)	128.7(4)	C(24)−N(4)−C(26)	123.6(4)
Cu−N(3)−C(25)	125.8(4)	C(25)−N(3)−C(23)	105.5(5)

Relative integration of the isotropically shifted signals in the NMR spectra of **2** and **4** indicates that all of them are generated by the same number of protons. The results of the elemental analysis performed on **2** and **4** suggest that each complex contains two CTZ (complex **2**) or two KTZ (complex **4**) ligands in their structures. Therefore, these ligands must be located in equivalent positions with respect to the metal centers in complexes **2** and **4**.

Crystal Structure of $[Cu(CTZ)_4]Cl_2$. A molecular diagram for the cation of compound **1** is shown in Figure 3, while selected bond distances and angles are collected in Table 3. The crystal structure shows (apart from the solvent molecule) half of the $Cu(CTZ)_4^{2+}$ cation and a chloride anion as crystallographically independent molecular fragments in the asymmetric unit. The copper located in a center of symmetry and four nitrogen atoms lie in the same plane leading to a perfect planar configuration. However, the bond angles N(1)−Cu−N(3) [92.0(2)°] and N(1)−Cu−N(3′) [88.0(2)°] show a small deviation from the square arrangement. The bond distances Cu−N(1) 2.013(4) Å and Cu−N(3) 1.996(4) Å are typical for tetrakis(imidazole)copper(II) complexes.[26] The dihedral angles between the N1C1N2C2C3 and N3C23N4C24C25 imidazole planes and the equatorial CuN_4 unit are 77.1 and 77.8°, respectively. These structural features are similar to those reported for tetragonal $[Cu(1,4,5\text{-tmi})_4][ClO_4]_2$[27] (tmi = trimethylimidazole). In the crystal structure of **1** two chloride anions are symmetrically located in both apical positions of discrete $Cu(CTZ)_4^{2+}$ cations at a Cu···Cl distance of 2.998 Å suggesting a weak interaction between these two atoms. This Cu···Cl distance is longer than the Cu−Cl bond distances (2.250 Å) previously reported for four-coordinate Cu(II) complexes.[28]

Synthesis and Characterization of Gold Complexes. Two new gold complexes $[Au(PPh_3)(CTZ)]PF_6$ (**5**) and $[Au(PPh_3)(KTZ)]PF_6 \cdot H_2O$ (**6**) were synthesized by reaction of $AuClPPh_3$ with KPF_6 in acetonitrile to remove the coordinated chloride, after which the CTZ or KTZ ligand was added. We have previously employed a similar procedure for the preparation of $[Au(PPh_3)(CQ)]PF_6$ (CQ = chloroquine).[9]

These compounds were obtained as air stable white solids whose elemental analyses are in agreement with the molecular formula $[Au(PPh_3)(L)]PF_6$ (L = CTZ or KTZ). The infrared spectrum of complex **5** showed the signals corresponding to the aromatic C−H stretching at 3050 cm^{-1}, the C═N stretching at 1500 cm^{-1}, and the C═C stretching at 1453 cm^{-1}. The IR spectrum of complex **6** showed signals corresponding to the stretching vibrations: C−H (aromatic) at 3150 cm^{-1}; C−H(aliphatic) at 2920 cm^{-1}; C═O at 1643 cm^{-1}; C═C at 1517 cm^{-1}; C═N at 1445 cm^{-1}; C−O−Ar at 1200 cm^{-1}. All these signals are slightly shifted with respect to those shown by the free ligands. The IR spectra also showed the characteristic signal due to the P−F stretching at 843 cm^{-1} for the PF_6^- counterion.

The $^{31}P\{^1H\}$ NMR spectra for $[Au(PPh_3)(CTZ)]PF_6$ and $[Au(PPh_3)(KTZ)]PF_6 \cdot H_2O$ exhibit singlet signals corresponding to PPh_3 at 27.9 ppm and at 28.3 ppm, respectively, which are 3.1 and 2.7 ppm shifted to highfield with respect to the chemical shift in the parental gold compound ($AuClPPh_3$). These spectra also showed the characteristic PF_6^- signal, as a heptuplet centered at 145.5 ppm with a coupling constant J_{P-F} = 713 Hz. The ^1H NMR chemical shifts of the imidazole protons H2, H4, and H5, which are displaced downfield with respect to the free ligand, are shown in Table 4. This indicates that CTZ or KTZ are coordinated to gold in both complexes **5** and **6** through the imidazole nitrogen atom of each ligand. Additionally, the relative integral of the signals for the phenyl protons of PPh_3 in these spectra are in agreement with a PPh_3:L ratio of 1:1 in each complex. The structures of **5** and **6** that correspond to a 14-electron configuration for Au(I) are most probably in the typical linear coordination geometry[29] which has been previously associated with biological activity.[6,7]

Biological Activity. The effect of the new complexes **1**−**6** on the proliferation of in vitro cultures of the epimastigote form of *T. cruzi* was evaluated as described in the Experimental Section; Table 5 summarizes the results of such tests. Since the number of CTZ or KTZ ligands vary from one complex to another, to allow direct comparisons, the experiments were

(26) (a) Farida, A.; Goodgame, D. M. L.; Goodgame, M.; Rayner-Canham G. W.; Skapski, C. A. *Chem. Commun.* **1968**, 757−61. (b) McFadden, D. L.; McPhail, A. T.; Garner, C. D.; Mabbs, F. E. *J. Chem. Soc., Dalton Trans.* **1976**, 47−52.

(27) Bernarducci, E.; Bharadwaj, P. K.; Krogh-Jespersen, K.; Potenza, J. A.; Schugar, H. J. *J. Am. Chem. Soc.* **1983**, *105*, 3860.

(28) (a) Biagini Cingi, M.; Bigoli F.; Lanfranchi, M.; Pellinghelli M. A.; Vera, A.; Buluggiu, E. *J. Chem. Soc., Dalton Trans.* **1992**, *21*, 3145. (b) Raithby, P. R.; Shields, G. P.; Allen, F. H.; Samuel Mortherwell, W. D. *Acta Crystallogr., Sect. B* **2000**, *56*, 444−454.

(29) Shroder, M.; Stephenson, T. A. *In Comprehensive Coordination Chemistry*; Wilkinson, G., Gillard, R. D., McCleverty, J. A., Eds.; Pergamon: Oxford, U.K., 1987; Vol. 2, Chapter 15.

Table 4. Selected ^{1}H and ^{31}P NMR Data for Gold Complexes

	^{1}H NMR [δ/ppm ($\Delta\delta$)]			
compd	H2	H4	H5	^{31}P NMR [δ/ppm ($\Delta\delta$)] for PPh_3
$[Au(CTZ)PPh_3]PF_6$	7.91 (0.47)	7.36 (0.33)	7.01 (0.28)	27.9 (3.1)
$[Au(KTZ)PPh_3]PF_6$	8.25 (0.77)	7.20 (0.25)	7.06 (0.13)	28.2 (2.8)

Table 5. Effect of CTZ, KTZ, and Their Cu and Au Complexes on the Proliferation of the Epimastigotes of *T. Cruzi*[a]

compd	% inhibition
CTZ	0
KTZ	39
$[Cu(CTZ)_4]Cl_2$ (**1**)	66
$[Cu(CTZ)Cl_2]_2$ (**2**)	67
$[Cu(KTZ)_3]Cl_2$ (**3**)	73
$[Cu(KTZ)Cl_2]_2$ (**4**)	69
$[Au(CTZ)PPh_3]PF_6$ (**5**)	66
$[Au(KTZ)PPh_3]PF_6$ (**6**)	71

[a] Complexes were used as DMSO solutions of 1 μM (concentration based on the ligands). For details, see Experimental Section.

conducted by use of DMSO solutions of the complexes providing in each case a total concentration of 10^{-6} M of CTZ or KTZ in the growth medium. In general, the activities of the new metal derivatives were all considerably higher than those exhibited by the free ligands. The marked enhancement in the efficacy of CTZ by complexation to metals is demonstrated by the fact that, at 10^{-6} M, no effect on growth was observed with the free ligand, while the same concentration of the imidazole bound to copper or gold in the complexes induced over 66% growth inhibition. In the case of KTZ, the activity increases from 39% inhibition for the free ligand to over 70% inhibition for the complexes. These results can be considered as important improvements to previously known activities against *T. cruz*i, and they are consistent also with our published data with ruthenium complexes which provide growth inhibition of up to 82% at the same concentration.[3a] It is interesting to note also that the enhancement of the activity of the free ligands reported in Table 5 is not markedly influenced by the number of ligands attached to a single metal center, to the monomeric or dimeric nature of the copper complexes, or even to the nature of the metal ion.

We cannot at this moment offer a satisfactory explanation for this observation, but these results are reminiscent of the situation found for 1,2-bis(diphenylphosphino)ethane complexes of Cu, Ag, and Au, all of which display anticancer activities very similar to each other and to that of the free diphosphine; this has been interpreted in terms of the phosphine ligand itself being the anticancer agent, while the metal ions would be acting as protectors of the ligand against oxidation to the corresponding phosphine oxide which is known to be ineffective.[30] The possibility that in our case the CTZ and KTZ ligands are merely been protected against some deactivation process by the metal ions cannot be entirely ruled out, but it seems less likely, since the difference in activity with respect to the free ligands in this case and other previously reported examples[3] are notable. Moreover, preliminary studies on the possible mechanisms of action of these metal−azole complexes,[3b] as well as further experiments which are currently in progress in our laboratories, indicate a complex reaction scheme involving multistep hydrolytic processes, coupled with ligand exchange reactions leading to strong interactions of the metal ions with the DNA of the parasite. Hopefully these studies will shed more light on the influence of the metal and the structure of the complexes on the biological activity and, thus, allow us to improve the potential of these novel agents in a rational manner.

Conclusion

Here we have reported the synthesis and characterization of new Cu(II)−CTZ and Cu(II)−KTZ as well as Au(I)−CTZ and Au(I)−KTZ complexes. The characterization of these complexes was achieved through NMR, EPR, IR, UV−vis, elemental analysis, and X-ray diffraction. The biological activity of these complexes against the epimastigote form of *T. cruzi* was also evaluated indicating that all of them exhibit improved activity on parasite proliferation when compared with the free ligands.

Acknowledgment. CONICIT is gratefully acknowledged for the acquisition of the NMR spectrometer through the National NMR Laboratory at IVIC and for funding to M.N. through Project S1-98000945 and to R.A. through Project S1-96001062. This work was also supported by the UNDP/World Bank/World Health Organization Program for Research and Training in Tropical Diseases (Grant 9990201 to J.A.U.).

Supporting Information Available: X-ray data in the form of CIF files. This material is available free of charge via the Internet at http://pubs.acs.org.

IC0103087

(30) Lippard, S. J. In *Bioinorganic Chemistry*; Bertini, I., Gray, H. B., Lippard, S. J., Valentine, J. S., Eds.; University Science Books, Sausalito, CA, 1994; Chapter 9, p 520.